DOI 10.1002/pmic.201600036 *Proteomics* 2016, *16*, 1718–1725

RESEARCH ARTICLE

MALDI-MSI for the analysis of a 3D tissue-engineered psoriatic skin model

Amanda Harvey[1], Laura M. Cole[1], Rebecca Day[1], Maggie Bartlett[2], John Warwick[2], Richard Bojar[2], David Smith[1], Neil Cross[1] and Malcolm R. Clench[1]

[1] Centre for Mass Spectrometry Imaging, Biomolecular Sciences Research Centre, Sheffield Hallam University, Sheffield, UK
[2] Innovenn, Sand Hutton Innovation Campus, York, UK

MALDI-MS Imaging is a novel label-free technique that can be used to visualize the changes in multiple mass responses following treatment. Following treatment with proinflammatory cytokine interleukin-22 (IL-22), the epidermal differentiation of Labskin, a living skin equivalent (LSE), successfully modeled psoriasis in vitro. Masson's trichrome staining enabled visualization and quantification of epidermal differentiation between the untreated and IL-22 treated psoriatic LSEs. Matrix-assisted laser desorption ionization mass spectrometry imaging was used to observe the spatial location of the psoriatic therapy drug acetretin following 48 h treatments within both psoriatic and normal LSEs. After 24 h, the drug was primarily located in the epidermal regions of both the psoriatic and nonpsoriatic LSE models whereas after 48 h it was detectible in the dermis.

Received: January 22, 2016
Revised: May 5, 2016
Accepted: May 23, 2016

Keywords:
Acetretin / Interleukin-22 / Living skin equivalent / MALDI-MSI / Psoriasis / Skin / Tissue engineering / Technology

1 Introduction

Tissue engineering has enabled the development of skin models. These living skin equivalents (LSEs), derived from primary human skin cells, self-assemble to form stratified layers comparable to human skin [1–8]. LSEs offer treatment for burns patients following serious injury, avoiding the need for meshed skin grafts and donor skin [6–9]. Additionally, LSEs are used for toxicity screening with the ability to replace animal models for cosmetic and drug development. The use of skin models in drug development has been reviewed recently [10]. Whilst a 3D in vitro model would not be expected to show a full range of histopathological responses due to the absence of an immune system, blood supply, or innervation, LSE offers an alternative to animal models which can give useful data for studies, for example of drug absorption/penetration.

Correspondence: Professor Malcolm R. Clench, Centre for Mass Spectrometry Imaging, Biomolecular Sciences Research Centre, Sheffield Hallam University, Howard Street Sheffield, UK S1 1WB
E-mail: m.r.clench@shu.ac.uk

Abbreviations: ALI, air–liquid interface; **IL-22**, interleukin-22; **LSE**, living skin equivalent; **MSI**, mass spectrometry imaging

Psoriasis is a skin condition that causes red, flaky, crusty patches of skin covered with silvery scales or plaques that affects 2% of people in the United Kingdom (NHS 2015). One of the markers of psoriasis as an inflammatory disease is the interruption of normal cytokine pathways affecting cellular communication with keratinocytes. This interruption to the interleukin-22 (IL-22) pathway is one of the primary causes of adverse effects to these normal inflammatory pathways, which can cause keratin atherosclerosis, or thickening and unevening of the epidermis within patients with psoriasis, as shown in Fig. 1 [11–15]. Acanthosis in psoriasis is visible with the induction of psoriatic plaques on the skin surface. It is also responsible for the hypoproliferation of cells in the epidermis [16]. In this study, we have added IL-22 in order to induce psoriasis in vitro by mimicking the inflammatory response environment present [15–17].

One of the strengths of mass spectrometry imaging (MSI) is the ability to visualize the distribution of multiple compounds within tissues simultaneously and in a label-free manner [18]. We have previously applied MALDI-MSI to the study of both ex vivo human skin and 3D skin models [19–23]. MSI

Color Online: See the article online to view Figs. 1–5 and 7 in color.

Significance of the study

The work reported here represents the first reported mass spectrometric study of a 3D skin model modified to represent a disease state.

has recently been used to examine drug absorption in LSE, with the aim to identify the metabolism of drugs within LSE [24]. MALDI-MSI is continuing to grow as a robust technique for the analysis of tissues and offers great prospects for tissue engineering to compare the profile of native tissues and diseases with those of their tissue-engineered counterparts, overall enabling greater development of the latter.

In the study reported here, we have added IL-22 to a developing LSE in order to induce psoriasis in vitro by mimicking the inflammatory response environment present. We have examined the effects of the IL-22 treatment on both the structure of the LSE and the barrier function by the use of MALDI-MSI.

2 Materials and methods

2.1 Psoriatic development and LSE culture

LSE skin models at day 7 air–liquid interface (ALI; Labskin, Innovenn, York, UK) were treated with IL-22 (R&D Systems) for 14 days to induce psoriasis. Labskin maintenance medium (Innovenn, York, UK) was supplemented with IL-22 (10 ng/mL) and medium was refreshed daily keeping the LSEs at ALI. The epidermal differentiation and metabolic activity were monitored by AlamarBlue® staining every 2 days. Psoriasis drug treatments of topical acetretin (30 μL of 300 μg/mL in acetone/olive oil 4:1) were applied on day 21 and the efficacy and drug penetration within the skin models was compared over 48 h.

2.2 Fresh frozen tissue and cryosectioning

Directly following drug treatment, LSEs were removed from the well insert and snap frozen in a bath of precooled isopentane (2–5 min) in a Styrofoam box containing liquid nitrogen and a suitable float. LSEs were stored at −80°C for at least 24 h before sectioning. LSEs were mounted onto cork rings with dH_2O at −25°C and allowed to equilibrate to temperature for 30 min before being cryosectioned at 12 μm and freeze-thaw mounted onto "polycat" microscope slides (SLS, Hessle, UK).

2.3 Hematoxylin and eosin staining

LSE sections were stained using Mayers hematoxylin (VWR) and aqueous eosin Y (VWR) solutions. Each slide was submerged in hematoxylin for 8 min, washed in running tap water for 4 min, submerged in eosin y solution for 30 s, dH_20 for 1 min, and mounted with DPX (distyrene, a plasticizer, and xylene used as a synthetic resin mounting media) following dehydration through a series of alcohol and xylene dehydration baths. Slides were imaged using an Olympus BX60 microscope fitted with UPlanFl 10x/0.30, 20x/0.50 ∞/0.17, 40x/0/75 ∞/0.17 objectives and analyzed with QCapture-Pro 8.0 software (QImaging, Surry, BC, Canada).

2.4 Masson's trichrome staining

LSE sections were stained using Masson's trichrome staining kit (VWR). Slides were submerged in hematoxylin for 10 min, washed in running tap water for 4 min, stained in

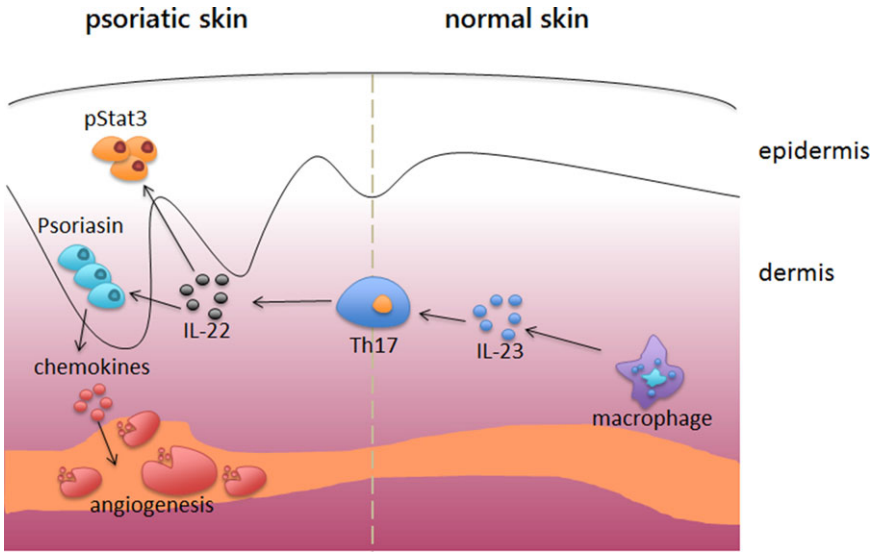

Figure 1. Simplified schematic of the changes that occur within skin in response to treatment with IL-22. Generally in psoriatic patients a specific stimulus will induce a cascade of events within skin culminating with the characteristic disregulated epidermis or acanthosis. The IL-23 produced by macrophages within the skin lead to immune responses of Th17 which produces the IL-22 of interest to this study. IL-22 in turn is responsible for the characteristic changes in the epidermis visible through the activation of pStat3 and psorasin, culminating with the production of chemokines, which leads to angiogenesis. Figure adapted [15].

ponceau fuchsin for 5 min, rinsed in dH_2O, submerged in phosphomolybdic acid for 3 min, and colored without rinsing in vert lumiere, before being rinsed in two baths of acidified water to remove excess dye. Following staining samples were mounted with DPX following dehydration through a serious of alcohol and xylene dehydration baths. Slides were imaged using an Olympus BX60 microscope fitted with UPlanFl 10x/0.30, 20x/0.50 ∞/0.17, 40x/0.75 ∞/0.17 objectives and analyzed with QCapture-Pro 8.0 software (QImaging). Epidermal thickness was measured from recorded images using ImageJ (https://imagej.nih.gov/ij/) and statistical analyses were carried out using StatsDirect (StatsDirect, Cheshire, UK). A Tukey analysis of variance was performed on multiple measurements taken from random sections, taken from treated and untreated LSEs.

2.5 Immunohistochemistry

Fresh frozen tissue sections were fixed in ice-cold acetone and endogenous peroxidases quenched. Antigen retrieval was performed in a microwave oven in 0.05 M Tris, pH 9.5. Samples were blocked in rabbit serum, then incubated overnight at 4°C with mouse anti-human Psoriasin (1:200; Abcam, ab13680) and with preimmune mouse IgG (Abcam) as a negative control (1:50). After washing, samples were incubated with biotinylated rabbit anti-mouse secondary antibody (1:500; Abcam) and binding detected by formation of streptavidin–biotin complexes (Vector Laboratories, Peterborough, UK) with 3,32-diaminobenzidine tetrahydrochloride solution (Sigma–Aldrich). Sections were counterstained with Mayers Hematoxylin (Leica Microsystems), dehydrated, cleared, and mounted in Pertex (Leica). Sections were visualized and images captured on an Olympus BX60 Microscope using QCapture Pro version 8.0 software (Media Cybernetics, Marlow, UK).

2.6 Small-molecule MALDI-MS imaging

For small-molecule MALDI-MS imaging, sections were coated with MALDI matrix (α-cyano-4-hydroxycinnamic acid, 5 mg/mL in 70:30 methanol: 0.5% TFA) using a SunCollect (SunChrom Friedrichsdor, Germany) sprayer. Slides were coated with four layers of CHCA matrix, spraying each layer approximately 50 μL per layer at 2 μL/min. Mass spectra and images were acquired in positive ion mode on an Applied Biosystems/MDS Sciex hybrid quadrupole TOF mass spectrometer (Q-Star Pulsar-i) with an orthogonal MALDI ion source (Applied Biosystems, Foster City, CA, USA) and a high-repetition neoddymium-doped yttrium aluminium garnet (Nd:YAG) laser (355 nm, 1 KHz) (Applied Biosystems). Image acquisition was performed at a spatial resolution of 100 μm × 100 μm in "Raster Image" mode; images were generated using the freely available Novartis Biomap 3.7.5.5 software (www.maldi-msi.org). Post-MS imaging sections were also examined by histology as described in this section.

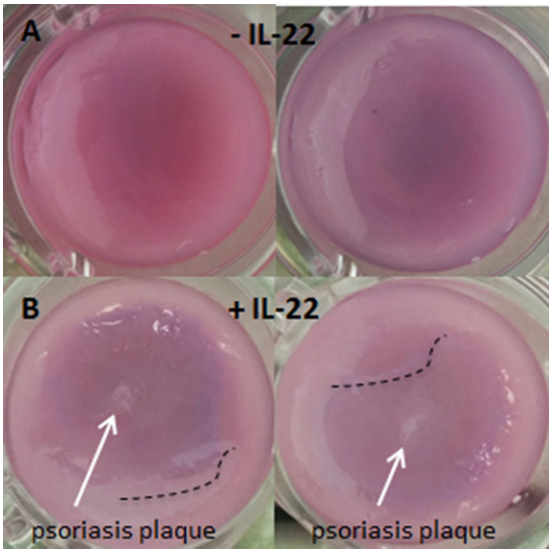

Figure 2. Labskin stained with AlamarBlue® at day 21 ALI. (A) Without treatment with IL-22 there are no visible changes to the epidermis of the LSEs. (B) LSEs treated with IL-22 show disregulation to the epidermis (dotted line) and psoriatic plaques (arrows) after treatment.

3 Results and discussion

3.1 Psoriatic development within LSEs

Following treatment with IL-22 from day 7 ALI for 2 weeks to day 21 ALI, psoriatic plaques were visible on the LSE constructs as shown in Fig. 2B (arrows). Costaining with AlamarBlue® highlighted abnormalities in epidermal differentiation within the LSE constructs visible by deregulation of the epidermal layer (acanthosis) visible in Fig. 2B (dashed lines) with IL-22 as contrasted with the smooth epidermal layer observed in Fig. 2A. The formation of this acanthosis within the epidermis of the treated LSEs creates a similar structure to that observed with in vivo psoriasis.

Standard H&E staining of the LSEs yielded results indicating thickening of the epidermis. In Fig. 3D following treatment with IL-22, it is possible to see an upper epidermal thickness of ~85 μm as opposed to ~32 μm in Fig. 3B without treatment of IL-22. Additionally, the character of the LSEs becomes quite characteristically wavy (i.e. exhibits disregulation) in Fig. 3C following treatment with IL-22 as opposed to Fig. 3A without.

Since standard H&E staining does not quantitatively enable measurement of the epidermal stratification, Masson's trichrome staining was performed to aid visualization of keratin and collagen within the layers of the epidermis allowing better measurements to be acquired. In Fig. 4A and B, it is

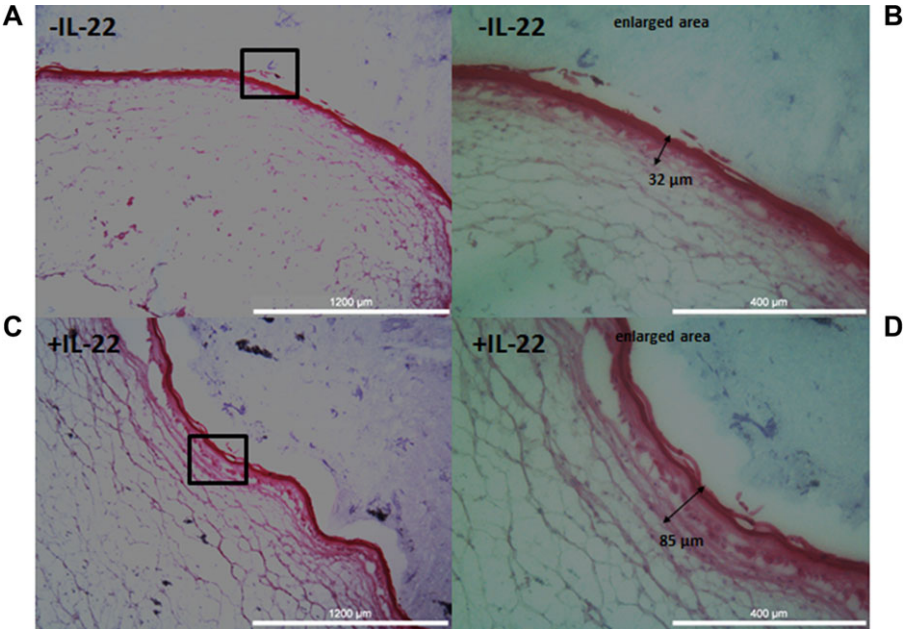

Figure 3. Histology H&E staining of Labskin at day 21 ALI. (A) Non-IL-22 treated LSE, "normal skin." (B) Enlarged area showing the measurable upper epidermal thickness of non-IL-22 treated LSE to be 32 µm. (C) IL-22 treated LSE, "psoriatic skin," characterised by wavy acanthosis. (D) Enlarged area showing the measurable upper epidermal thickness of IL-22 treated LSE to be 85 µm.

clear that there is very little stratification of the epidermis and its structure is fairly flat, however in Fig. 4C and D, the "wavy" psoriatic characteristic is clearly observable. The measured total epidermal thickness (comparing Fig. 4B and D) has increased from approximately 132 ± 14.6 µm to 179 ± 13.6 µm ($p = 0.01$), i.e. the thickening is statistically significant. The measured epidermal stratification of non-IL-22 treated Labskin is 41 ± 5.9 µm and for the treated samples 78 ± 21.6 µm ($p = 0.0568$), i.e. the difference is not statistically different.

In order to validate the psoriatic-like nature of the IL-22 treated LSE, immunohistochemical staining for the presence of psoriasin was carried out. As can be seen in Fig. 5, psoriasin is detectable in low abundance in untreated Labskin (Fig. 5A) but is much more highly expressed in the IL-22 treated samples (Fig. 5C). There is little indication of non-specific binding as shown by the specific isotype controls (Fig. 5B and D). Figure 5C also shows the epidermal thickening observed in both the H&E and Masson's stained samples.

3.2 Drug treatment of LSEs and analysis with MALDI-MSI

Acetretin, a psoriatic drug was chosen for its known effect toward psoriatic skin [25] and also for the ability of the drug to be visualized by MSI. The phosphatidylcholine head group (*m/z* 184) was chosen to enable visualization of the LSE structure as phospholipids are abundant in tissues such as skin. The positive phospholipid head group is key to their ionization efficiency. Figure 6A–F show representative LSE samples, Fig. 5A control without drug, Fig. 6B drug treated without IL-22 (24 h posttreatment), Fig. 6C IL-22 treated, drug-treated psoriatic LSE (24 h posttreatment) with Fig. 6E–F showing enlarged areas of these samples. In the enlarged images focusing on the epidermis of the LSEs, drug was not observed within the untreated control, Fig. 6D, as expected. The "red" drug signal is, however, clearly observable in the representative images of treated samples (Fig. 6E and F). The red acetretin signal (*m/z* 326.2) appears to be solely located within the epidermis, by comparison with the H&E image. From these images the depth of penetration of the drug into the LSE can be evaluated. For the non-IL-22 treated Labskin (Fig. 6E) the apparent depth of penetration is 114 µm and for the IL-22 treated Labskin (Fig. 6F) the apparent penetration is 177 µm, an increase of approximately 63 µm. This is in agreement with the previously measured (Fig. 4) epidermal stratification. Therefore at the 24 h time point, the distance penetrated appears to correspond to the thickness of the epidermis.

A 48 h posttreatment sample was imaged to examine drug distribution following longer treatment (Fig. 7). In this case a sodiated sphingomyelin (SM 34:1 $[M+Na]^+$) at *m/z* 725.4 was chosen to visualize the epidermis. In Fig. 7A, the epidermal regions of the various LSEs can be clearly seen. In this case, images were taken of LSEs with and without acetretin drug treatment and both with and without IL-22 treatment. In these preliminary results it is not possible to see a significant difference in the thickness of the epidermis using MSI of sphinogomyelins at the 100 µm spatial resolution used. Figure 7B shows a closer look at the LSE treated with both IL-22 and acetretin. Figure 7B shows the distribution of the *m/z 326.2* acetretin drug signal within the LSE. It is possible to see that after 48 h the drug has been effectively delivered

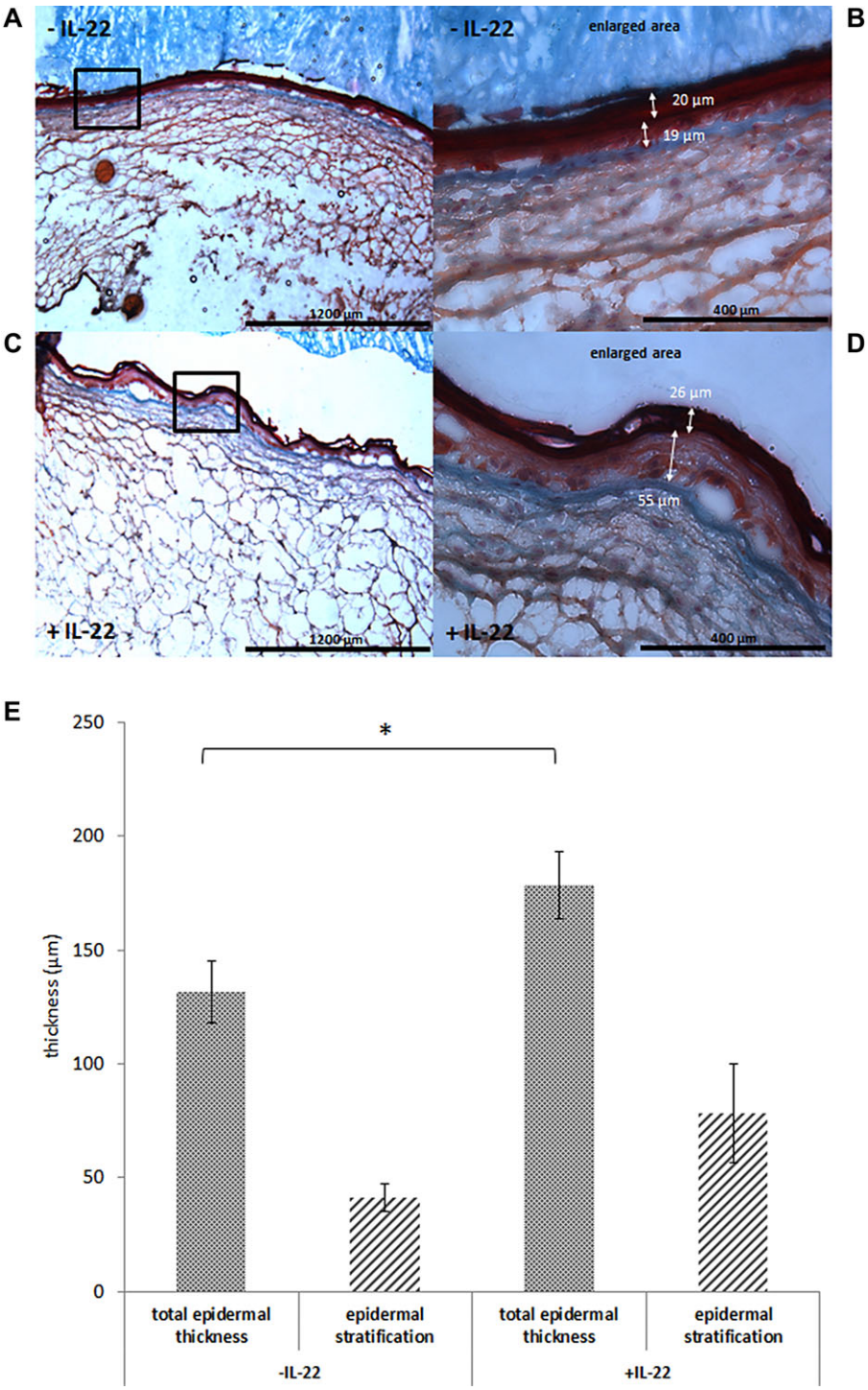

Figure 4. Histology Masson's Trichrome staining of Labskin at day 21 ALI. (A) Non-IL-22 treated LSE, "normal skin." (B) Enlarged area showing the measurable *stratum corneum* thickness of non-IL-22 treated LSE as 20 µm and stratification of the epidermal region of 19 µm. (C) IL-22 treated LSE, "psoriatic skin," characterised by wavy acanthosis. (D) Enlarged area showing the measurable *stratum corneum* thickness of IL-22 treated LSE as 26 µm and stratification of the epidermal region of 55 µm. (E) Statisical analysis of epidermal thickening observed in IL-22 treated and untreated Labskin ($p = 0.01$).

through the epidermis of the LSE into the dermal region with now an apparent depth of penetration of approximately 557 µm, the full thickness of the LSE.

Tissue engineering, and specifically skin tissue engineering has far from reached its limits. While much work was undertaken in the 1980–2000s to develop 3D culture of cells, and specifically tissue-engineered skin only recently have diseased models of skin been developed. Psoriasis has been linked very clearly with IL-22 pathway and as such IL-22-transformed psoriatic LSEs are effective ways to model the disease [15, 26]. IL-22 is responsible for activation of psorasin and pStat3 within the epidermis; these markers are visible by

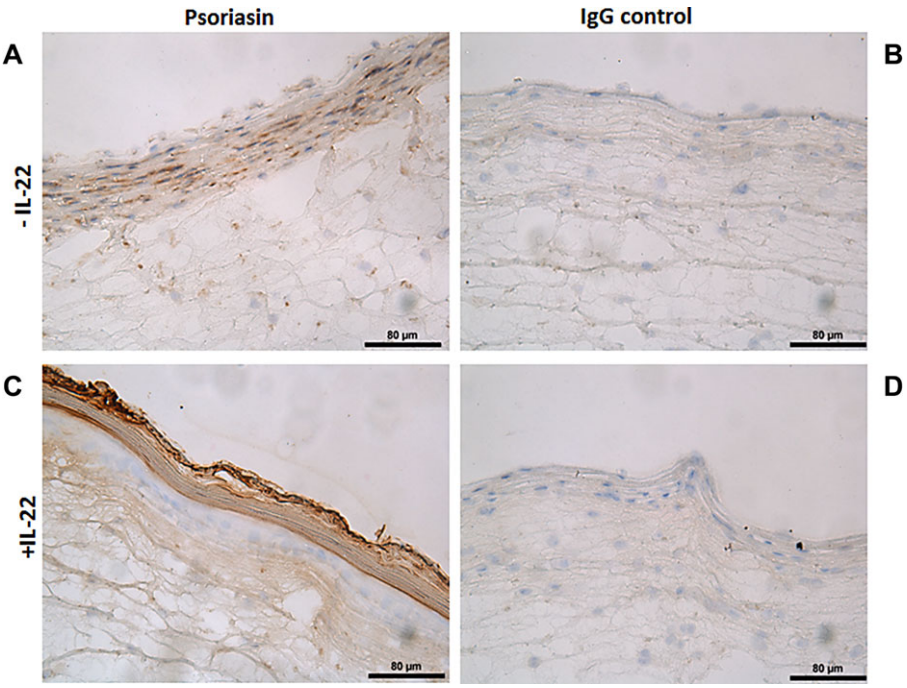

Figure 5. (A–D) Immunohistochemistry showing Psoriasin expression and localization in LabSkin. DAB staining (brown) shows Psoriasin is localized to the epidermal layers of the LSE model (A and C). LabSkin treated with IL-22 has a thickened epidermis and increased expression of Psoriasin (C).

immunohistochemistry and may be visible by MALDI-MSI. As with many diseases much of the specific mechanisms of psoriasis are still greatly unknown, and observing the presence of lipids, cytokines, chemokines, proteins, and peptide markers associated with the disease would greatly impact our understanding of the disease. This is therefore an ideal area for further study using MSI.

4 Concluding remarks

In this study we have been able to produce in vitro LSE models of psoriasis using Labskin commercial LSE, as confirmed by histology and have used MSI to determine the special location of the psoriatic drug acetretin. It was possible to demonstrate that 24 h posttreatment, the acetretin was located

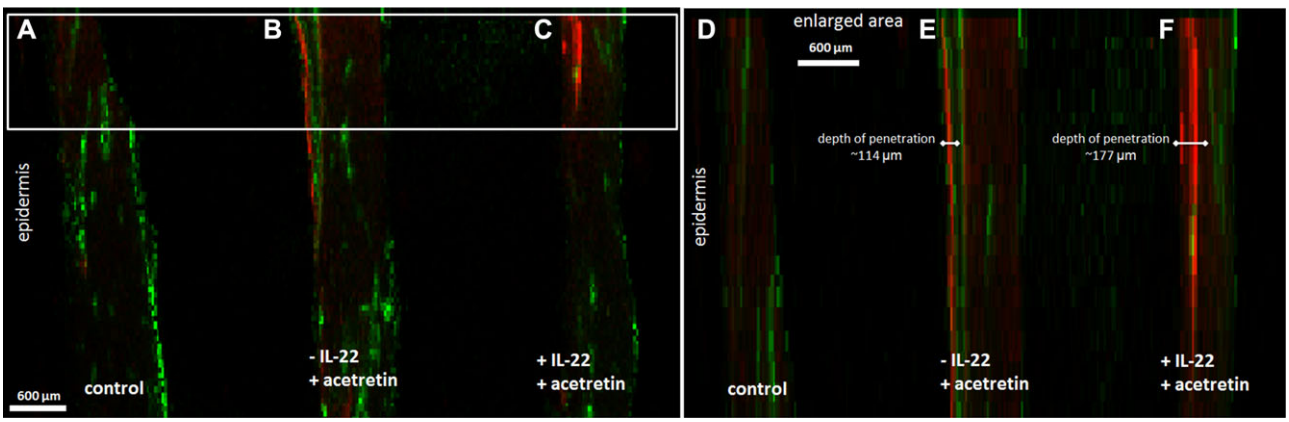

Figure 6. MALDI-MSI data overlay of *m/z* 326.2 acetretin (red) on *m/z* 184 phosphatidylcholine lipid (green) of LSEs 24 h posttreatment. (A) Non-IL-22 and nondrug-treated control. (B) Non-IL-22 and acetretin drug treated. (C) IL-22 and acetretin treated. Location of the drug is visible in the epidermis of treated samples. (D–F) Enlarged areas enable measurement of apparent depth of penetration of acetretin in the epidermal regions. (D) No drug signal present in the control. (E) The apparent depth of penetration within the non-IL-22 treated LSE is 114 µm. (F) The apparent depth of penetration within the IL-22 treated psoriatic LSE is 177 µm. The apparent larger abundance of drug within the psoriatic (+IL-22) LSE at 24 h posttreatment is explainable by the thicker epidermal region (63 µm increase in penetration depth).

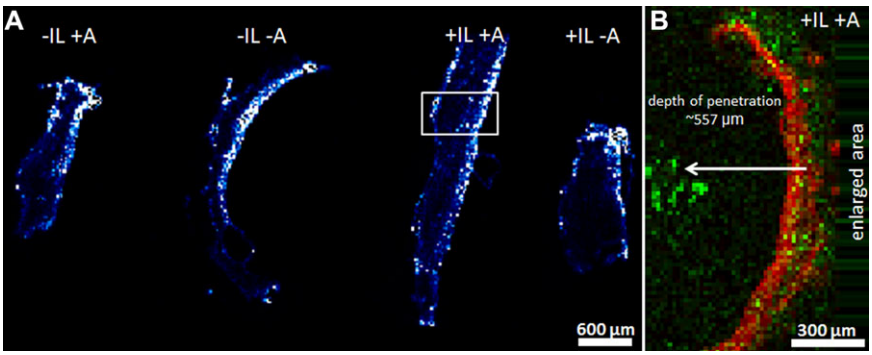

Figure 7. (A) MALDI-MSI distribution of sodiated sphingomyelin (SM 34:1 $[M+Na]^+$) at *m/z* 725.4 of LSEs 48 h posttreatment across all treatment samples. (B) Enlarged area MALDI-MSI data overlay of *m/z* 326.2 acetretin (green) on sodiated sphingomyelin (SM 34:1 $[M+Na]^+$) at *m/z* 725.4 of LSEs 48 h posttreatment. Apparent acetretin depth of penetration is 557 µm, i.e. it has penetrated to within the dermal region.

in the epidermal region in both psoriatic and nonpsoriatic skin models whereas 48 h posttreatment it had penetrated into the dermis.

We intend to utilize sphingomyelins (or different lipid, peptide, or protein species) in combination with matrix sublimation to obtain high-resolution images of the epidermal region of the LSE model in future studies.

This work was funded by NC3Rs Grant No. NC/L001896/1. The authors would also like to express their gratitude to the technical team at Innovenn for helping to provide the Labskin LSEs.

The authors have declared no conflict of interest.

5 References

[1] Groeber, F., Holeiter, M., Hampel, M., Hinderer, S. et al., Skin tissue engineering–in vivo and in vitro applications. *Adv. Drug Deliv. Rev.* 2011, *63*, 352–366.

[2] MacNeil, S., Progress and opportunities for tissue-engineered skin. *Nature* 2007, *445*, 874–880.

[3] Priya, S. G., Jungvid, H., Kumar, A., Skin tissue engineering for tissue repair and regeneration. *Tissue Eng. Part B Rev.* 2008, *14*, 105–118.

[4] Lu, G., Huang, S., Bioengineered skin substitutes: key elements and novel design for biomedical applications. *Int. Wound J.* 2013, *10*, 365–371.

[5] Yildirimer, L., Thanh, N. T. K., Seifalian, A. M. et al., Skin regeneration scaffolds: a multimodal bottom-up approach. *Trends Biotechnol.* 2012, *30*, 638–648.

[6] Auger, F. A., Berthod, F., Moulin, V., Pouliot, R. et al., Tissue-engineered skin substitutes: from in vitro constructs to in vivo applications Skin TE approaches. *Biotechnol. Appl. Biochem.* 2004, *39*, 263–275.

[7] MacNeil, S., Shepherd, J., Smith, L., in: , *3D Cell Culture: Methods and Protocols, Methods in Molecular Biology*, 2011, pp. 129–153.

[8] Bell, E., Parenteau, N., Gay, R., Nolte, C. et al., The living skin equivalent: its manufacture, its organotypic properties and its responses to irritants. *Toxicol. Vitr.* 1991, *5*, 591–596.

[9] Demling, R. H., DeSanti, L., Management of partial thickness facial burns (comparison of topical antibiotics and bio-engineered skin substitutes). *Burns* 1999, *25*, 256–261.

[10] Mathes, S. H., Ruffner, H., Graf-Hausner, U., The use of skin models in drug development. *Adv. Drug Deliv. Rev.* 2014, *69–70*, 81–102.

[11] Wolk, K., Haugen, H. S., Xu, W., Witte, E. et al., IL-22 and IL-20 are key mediators of the epidermal alterations in psoriasis while IL-17 and IFN-gamma are not. *J. Mol. Med.* 2009, *87*, 523–536.

[12] Hao, J. Q., Targeting interleukin-22 in psoriasis. *Inflammation* 2014, *37*, 94–99.

[13] Ma, H., Liang, S., Li, J., Napierata, L. et al., IL-22 is required for Th17 cell-mediated pathology in a mouse model of psoriasis-like skin inflammation. 2008, *118*, 597–607.

[14] Niv-Spector, L., Shpilman, M., Levi-Bober, M., Katz, M. et al., Preparation and characterization of mouse IL-22 and its four single-amino-acid muteins that act as IL-22 receptor-1 antagonists. *Protein Eng. Des. Sel.* 2012, *25*, 397–404.

[15] Danilenko, D. M., Review paper: preclinical models of psoriasis. *Vet. Pathol.* 2008, *45*, 563–575.

[16] Portugal-Cohen, M., Horev, L., Ruffer, C., Schlippe, G. et al., Non-invasive skin biomarkers quantification of psoriasis and atopic dermatitis: cytokines, antioxidants and psoriatic skin auto-fluorescence. *Biomed. Pharmacother.* 2012, *66*, 293–299.

[17] Rüffer, C., Psoriatic in vitro epidermis A human tissue culture model for testing cosmetical and medical skin care products. *Househ. Pers. Care Today* 2011, 30–33.

[18] Cornett, D. S., Reyzer, M. L., Chaurand, P., Caprioli, R. M. et al., MALDI imaging mass spectrometry: molecular snapshots of biochemical systems. *Nat. Methods* 2007, *4*, 828–833.

[19] Mitchell, C. A., Long, H., Donaldson, M., Francese, S. et al., Lipid changes within the epidermis of living skin equivalents observed across a time-course by MALDI-MS imaging and profiling. *Lipids Health Dis.* 2015, *14*, 84.

[20] Hart, P. J., Francese, S., Claude, E., Woodroofe, M. N. et al., MALDI-MS imaging of lipids in ex vivo human skin. *Anal. Bioanal. Chem.* 2011, *401*, 115–125.

[21] Hart, P. J., Francese, S., Woodroofe, M. N., Clench, M. R., Matrix assisted laser desorption ionisation ion mobility separation mass spectrometry imaging of ex-vivo human skin. *Int. J. Ion Mobil. Spectrom.* 2013, *16*, 71–83.

[22] Cole, L. M., Mahmoud, K., Haywood-Small, S., Tozer, G. M. et al., Recombinant " IMS TAG" proteins—a new method for validating bottom-up matrix-assisted laser desorption/ionisation ion mobility separation mass spectrometry imaging. *Rapid Commun. Mass Spectrom.* 2013, *27*, 2355–2362.

[23] Cole, L. M., Clench, M. R., Mass spectrometry imaging for the proteomic study of clinical tissue. *Proteomics Clin. Appl.* 2015, *9*, 335–341.

[24] Avery, J. L., McEwen, A., Flinders, B., Francese, S. et al., Matrix-assisted laser desorption mass spectrometry imaging for the examination of imipramine absorption by Straticell-RHE-EPI/001 an artificial model of the human epidermis. *Xenobiotica* 2011, *41*, 735–742.

[25] Hsia, E., Johnston, M. J., Houlden, R. J., Chern, W. H. et al., Effects of topically applied acitretin in reconstructed human epidermis and the rhino mouse. *J. Invest. Dermatol.* 2008, *128*, 125–130.

[26] Fernandes, I. R., Russo, F. B., Pignatari, G. C., Evangelinellis, M. M. et al., Fibroblast sources: where can we get them? *Cytotechnology* 2014, 1–6.

